Automated Homogeneity Inspection of U3O8-Al Dispersion Fuel Plates Using X-ray Radiography, Deep Learning and Chimp Optimization Algorithms

Authors: Elsharkawy, Prof. Zeinab Fathi, Fikry, Prof. Refaat Mohamed, Nawwar, Dr. Nadia, Ahmed, Prof. Amer Galal, Elbedawy, Dr. Mohammed ElSayed, Fikry, Prof. Refaat Mohamed

Date: 2025-09-23T16:51:59+00:00

Abstract

The uniform distribution of U3O8 particles within an aluminum matrix is crucial for the optimal performance and safety of plate-type nuclear fuel produced by the dispersion technique. X-ray radiography is one of the methods employed to inspect the homogeneity of U3O8-Al dispersion fuel plates. This non-destructive inspection technique involves an X-ray source emitting a beam that passes through the fuel plates, with varying absorption based on the material' s density. The resulting image reveals the internal distribution of U3O8 particles, allowing inspectors to identify any inhomogeneities. This study presents an automated inspection system combining deep learning and optimization algorithms to classify fuel plates into "Homogeneous"(regular) or "non-homogeneous" (observed/defected). Multiple optimization techniques are evaluated to identify the most effective approach, using the Chimp Optimization Algorithm (CHOA) that selected for its superior performance. Leveraging a pre-trained Efficient Net for feature extraction and CHOA for feature selection, the system identifies optimal discriminative features, while a support vector machine (SVM) classifier, optimized via CHOA, achieves classification accuracies of 99.77% (binary) and 99.72% (ternary) classification. This approach significantly improves inspection reliability and efficiency, ensuring robust nuclear fuel quality control.

Full Text

Automated Homogeneity Inspection of U O -Al Dispersion Fuel Plates Using X-ray Radiography, Deep Learning and Chimp Optimization Algorithms

Zeinab F. Elsharkawy[1], Refaat M. Fikry[1], Nadia M. Nawwar[1], A. G. Ahmed[2], Mohammed E. El-Bedawy[2]

[1] Engineering Department, Nuclear Research Center, Egyptian Atomic Energy Authority (EAEA), Egypt
[2] Nuclear Metallurgy Department, Nuclear Research Center, Egyptian Atomic Energy Authority (EAEA), Egypt

Abstract

The uniform distribution of U O particles within an aluminum matrix is crucial for the optimal performance and safety of plate-type nuclear fuel produced by the dispersion technique. X-ray radiography is one of the primary methods employed to inspect the homogeneity of U O -Al dispersion fuel plates. This non-destructive inspection technique involves an X-ray source emitting a beam that passes through the fuel plates, with varying absorption based on the material' s density. The resulting image reveals the internal distribution of U O particles, allowing inspectors to identify any inhomogeneities.

This study presents an automated inspection system combining deep learning and optimization algorithms to classify fuel plates as "homogeneous" (regular) or "non-homogeneous" (observed/defected). Multiple optimization techniques are evaluated to identify the most effective approach, with the Chimp Optimization Algorithm (CHOA) selected for its superior performance. Leveraging a pre-trained EfficientNet for feature extraction and CHOA for feature selection, the system identifies optimal discriminative features, while a support vector machine (SVM) classifier, optimized via CHOA, achieves classification accuracies of 99.77% (binary) and 99.72% (ternary). This approach significantly improves inspection reliability and efficiency, ensuring robust nuclear fuel quality control.

Keywords: X-ray radiography, U O -Al fuel plates, deep learning, Chimp Optimization Algorithm (CHOA), automated inspection, nuclear quality control

1. Introduction

Since 1998, the Fuel Manufactured Pilot Plant (FMPP) has been producing plate-type nuclear fuel for the Egyptian Second Research Reactor (ETRR-2). This fuel is a U O -Al dispersion fuel type (19.75% U^{23}). U O serves as a chemical compound that contains the fissile material (U^{23}) in nuclear fuel, typically dispersed within an aluminum matrix to form a composite material encased in cladding made from 6061 nuclear-grade aluminum alloy using the "picture frame" technique [1].

The distribution of U O within the aluminum powder matrix is a critical aspect of fuel performance during reactor operation. Uranium homogeneity refers to the uniform distribution of uranium within a nuclear fuel plate, which is essential for consistent fuel behavior, optimal reactor performance, and safety. The distribution of U O particles impacts heat generation along the fuel plate; inhomogeneities lead to localized hotspots, increasing local thermal stresses and risking fuel clad failure. Additionally, non-uniform distribution affects reactivity and neutron moderation, leading to reduced fuel efficiency and operational challenges [2, 3].

In the context of examining U O distribution uniformity, X-ray radiography provides a valuable tool for assessing the homogeneity of U O -Al dispersion fuel plates [4, 5]. In radiography, an X-ray source emits a beam of high-energy electromagnetic radiation that passes through the nuclear fuel plates and is absorbed in varying degrees based on the material' s density and thickness. The penetrating X-rays strike a detector (such as film or a digital sensor) on the opposite side. Areas with higher density (such as uranium oxide particles) absorb more X-rays, reducing intensity reaching the detector, while lower-density areas (such as the aluminum matrix) allow more X-rays to pass through. These intensity variations create an image representing the internal structure, enabling inspectors to examine U O particle distribution. Uniformly distributed particles appear as consistent patterns, while localized accumulations or inhomogeneities are visible as deviations from uniform distribution. The transmission densitometer is one tool used for this evaluation, measuring transmitted light intensities through a small circular aperture using a photoelectric sensor [6].

Examples of fuel meats with good and acceptable homogeneity are shown in Fig. 1

, representing reference radiographs based on field experience. Any variations in uranium density within specific areas of the fuel meat are reflected in densitometer readings corresponding to those regions. Statistical analysis of collected data is then performed to determine the homogeneity level in each plate [7].

X-ray radiography serves as a crucial non-destructive testing (NDT) technique for fuel plate inspection, capturing detailed internal images that reveal U O particle distribution within the aluminum matrix without physical alteration (Fig. 2

). While this technique offers critical insights into fuel homogeneity, traditional manual assessment presents significant challenges. Human-based inspection is time-consuming and suffers from subjectivity and declining accuracy in high-volume production. These limitations have driven adoption of machine learning (ML) and deep learning (DL)-based automated inspection systems, which demonstrate superior detection accuracy, processing speed, and consistency compared to conventional visual examination.

Recent advancements in computer vision and artificial intelligence show significant potential for automating defect detection and material characterization.

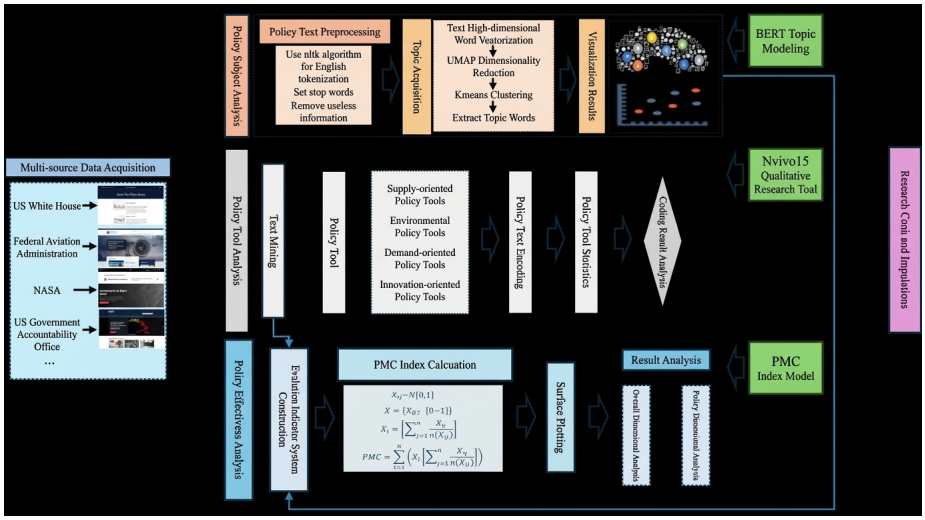

Figure 1: Figure 1

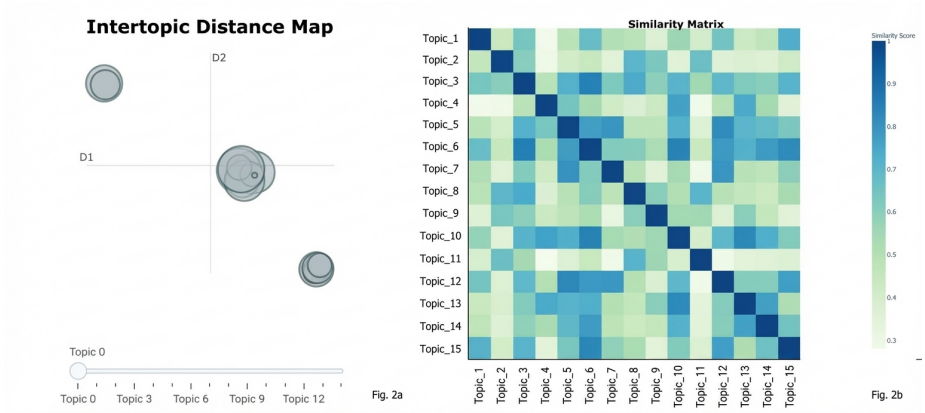

Figure 2: Figure 2

Deep convolutional neural networks (CNNs) [8, 9] can extract high-level features from radiography images for accurate defect classification. However, model effectiveness depends heavily on optimal feature selection and classifier optimization. Traditional dimensionality reduction techniques like Principal Component Analysis (PCA) and Linear Discriminant Analysis (LDA) [24] often struggle with high-dimensional data, while suboptimal hyperparameter tuning degrades performance. Metaheuristic optimization algorithms [10-16], such as the Chimp Optimization Algorithm (CHOA) [17-20], have shown remarkable success in enhancing ML models by efficiently navigating complex search spaces to identify optimal features and parameters.

Current nuclear fuel inspection systems face three fundamental limitations: (1) manual feature dependency in traditional GLCM-based approaches that restricts adaptability to novel defect types, (2) computational inefficiency of deep learning models that hinders real-time deployment, and (3) oversimplified binary classification frameworks that lack granularity for multi-defect analysis. To overcome these challenges, this study proposes an integrated framework combining EfficientNet-based deep feature extraction for robust pattern recognition, CHOA-optimized feature selection to enhance discriminative capability while maintaining computational efficiency, and CHOA-tuned SVM classification achieving superior accuracy in both binary (defective/non-defective) and ternary (regular/observed/defected) tasks, thereby addressing all three limitations simultaneously.

2. Related Work

Automated inspection of nuclear fuel plates has evolved significantly over the past two decades, leveraging advancements in non-destructive testing (NDT), image processing, and machine learning. This section reviews key methodologies for nuclear fuel inspection, focusing on X-ray radiography, texture analysis, deep learning, and optimization algorithms.

X-ray radiography has long served as a primary NDT method for evaluating U O -Al dispersion fuel plate homogeneity. Early approaches relied on manual expert inspection using transmission densitometers to measure radiographic film density variations correlated with uranium particle distribution [6, 7]. While effective, this method was labor-intensive and subjective, leading to inconsistencies in large-scale production.

To overcome manual inspection limitations, researchers increasingly adopted ML techniques. Early automated systems used texture analysis, with Keyvan et al. [21] exploring supervised neural networks (backpropagation and fuzzy ARTMAP) and unsupervised ART2-A for pellet inspection, finding supervised learning outperformed unsupervised methods. Berbar et al. [22] proposed a system using Haralick' s Gray Level Co-occurrence Matrix (GLCM) to extract textural features from U O -Al X-ray images, achieving 96% accuracy with a Backpropagation Neural Network (BPNN). However, this approach was limited

by handcrafted features that may not generalize to complex defects.

Recent studies have shifted toward DL for higher-accuracy defect detection. Guo et al. [23] applied Faster R-CNN with ResNet-101 to detect scratches on fuel assemblies, achieving 98% true positive rate at 10% false positive rate. These studies underscored DL potential while identifying challenges such as the need for large annotated datasets and computational resources.

The performance of ML-based inspection systems critically depends on optimal feature selection and model parameter tuning. While traditional techniques like PCA and LDA have demonstrated utility in simpler applications, their linear assumptions often fail to capture complex, nonlinear relationships in high-dimensional data. Metaheuristic optimization algorithms have emerged as powerful alternatives, including Whale Optimization Algorithm (WOA), Dragonfly Algorithm (DA) [11, 15], Salp Swarm Algorithm (SSA) [10, 15], Sine-Cosine Algorithm (SCA) [11, 15], and Grey Wolf Optimizer (GWO) [13-15]. Among these, CHOA has demonstrated particular efficacy due to superior convergence speed and balanced exploration-exploitation dynamics, making it especially suitable for high-dimensional optimization challenges in defect classification [17-20].

3. Methodology

The proposed system leverages EfficientNet-B0 as a deep feature extractor, followed by CHOA for feature selection to enhance discriminative capability while minimizing computational overhead. Subsequently, CHOA is utilized again to fine-tune SVM hyperparameters. This dual-stage optimization framework significantly boosts classification performance, achieving high accuracy in both binary (Hom/Non-Hom) and ternary (regular/observed/defected) tasks.

3.1 EfficientNet-B0

EfficientNet-B0 serves as an optimal feature extractor for nuclear fuel plate inspection, combining computational efficiency with robust pattern recognition [25-27]. As the baseline of the EfficientNet family, it employs compound scaling to balance depth, width, and resolution. The architecture consists of an initial 3×3 convolution followed by 16 MBConv layers (mixing 3×3/5×5 kernels) and global max pooling, outputting a 1280-D feature vector from raw images as shown in Fig. 3 [FIGURE:3].

With only 5.3M parameters, its pre-trained weights enable effective transfer learning, extracting hierarchical features directly from U O -Al radiographs without preprocessing or large datasets. The network's ability to capture multi-scale spatial patterns makes it ideal for nuclear fuel inspection tasks where defect manifestations vary significantly in size and morphology. By leveraging EfficientNet's deep feature representations, the system reduces reliance on manual feature engineering while improving defect detection robustness.

3.2 Hybrid CHOA-SVM Optimization Framework

The Chimp Optimization Algorithm (CHOA) is a population-based metaheuristic inspired by intelligent chimpanzee social and hunting behaviors [17-20]. It has demonstrated strong capabilities in global optimization and is particularly well-suited for high-dimensional search spaces, making it effective for feature selection and parameter tuning in machine learning tasks.

CHOA is employed in a two-stage hierarchical optimization process to enhance SVM performance for nuclear fuel plate defect classification. In Stage 1 (Feature Selection), CHOA operates on a binary-encoded population where each chimp represents a candidate feature subset. The fitness of each subset is evaluated by training an SVM with default parameters and measuring cross-validation accuracy. CHOA' s position update rules—modeling chimps' group hunting dynamics with chaotic exploration—iteratively refine feature subsets until convergence, effectively eliminating redundant or noisy features. Stage 2 (Parameter Optimization) then optimizes SVM hyperparameters (e.g., regularization strength C, kernel coefficient) using continuous-valued chimps, where fitness is assessed via cross-validation on the optimal feature subset identified in Stage 1. The algorithm' s adaptive chaos factor balances exploration of the parameter space with exploitation of promising regions. Finally, the selected features and tuned parameters are used to train a high-performance SVM classifier, achieving superior generalization by simultaneously addressing dimensionality reduction and model calibration. This hybrid approach leverages CHOA' s strengths in both discrete (feature selection) and continuous (parameter optimization) search spaces while maintaining computational efficiency through parallelizable fitness evaluations. The pseudo-code for the proposed Hybrid CHOA-SVM is shown in Fig. 4

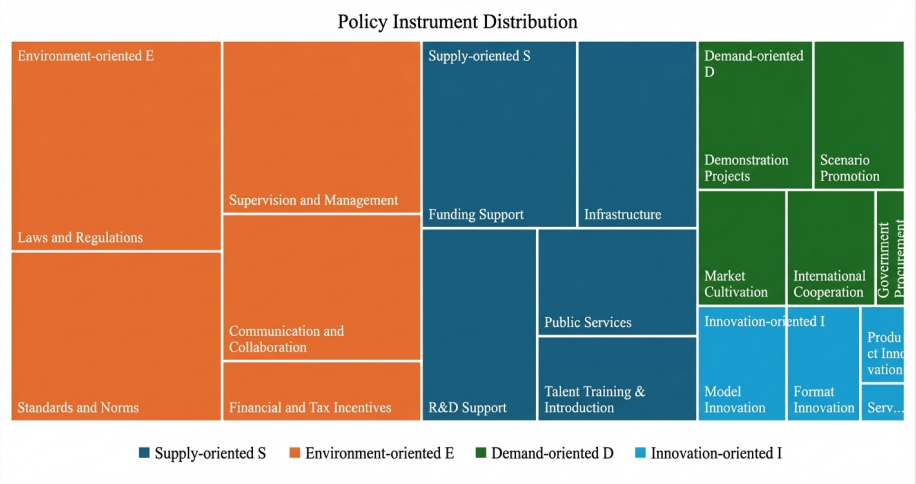

Figure 3: Figure 4

.

4. Experimental Results and Discussion

4.1 Data Description

Experiments were conducted using a dataset of fuel plate images manufactured for the ETRR-2 reactor. Classification was performed under two scenarios: binary (Homogeneous vs. Non-Homogeneous) and ternary (Regular, Observed, or Defected). Data augmentation techniques were applied to improve model generalization, including vertical and horizontal flipping, blurring, cropping, and random rotations (20° to 280°).

The binary classification task employed 4,330 images (2,570 homogeneous and 1,760 non-homogeneous), while the ternary classification used 3,570 images (1,810 regular, 1,496 observed, and 264 defected).

4.2 Evaluation Metrics

Classification accuracy (CA), confusion matrix (CM), area under the receiver operating characteristics curve (AUC), precision (P), specificity (Sp), recall (R), and F1-score (F1) are used to evaluate model performance:

- Precision: TP / (TP + FP)
- Recall: TP / (TP + FN)
- Specificity: TN / (TN + FP)
- F1-score: 2 × P × R / (P + R)
- Classification accuracy: (TP + TN) / (TP + TN + FP + FN)

where TP, FP, TN, and FN represent true positives, false positives, true negatives, and false negatives, respectively.

4.3 Results and Discussion

To attain optimal performance, the optimized SVM is fed with robust features acquired by CHOA. All experiments used consistent hardware: an Intel Core i7-10870H 8-core processor, 16GB RAM, and NVIDIA GeForce RTX 3060 GPU, running Windows 11 with MATLAB 2024a.

The CHOA framework was implemented with a population size of 50 chimps and 100 iterations. The dataset was partitioned into 90% for training (with 10-fold cross-validation) and 10% for testing. Deep features were extracted using EfficientNet-B0, followed by feature selection. Six metaheuristic algorithms—SSA, WOA, GWO, DA, SCA, and CHOA—were employed to optimize feature selection and SVM hyperparameters, with performance systematically compared.

Binary Classification Performance: As shown in Table 1 , CHOA achieved the most efficient feature selection, reducing the initial 1,028 features to only 191 (an 81.4% reduction) while yielding the highest classification accuracy for both feature selection and SVM optimization. Although SSA exhibited the highest

training accuracy, CHOA demonstrated superior testing performance and overall robustness. The confusion matrix and ROC curves further validate model effectiveness, as shown in Figs. 5 [FIGURE:5] and 6 [FIGURE:6]. Only one homogeneous plate image was misclassified, while all non-homogeneous images were correctly identified. AUC values of 1.0 for both classes confirm near-perfect classification performance.

Ternary Classification Performance: For the three-class scenario (Regular, Observed, Defected), CHOA again outperformed competing algorithms, selecting only 315 features while achieving the highest classification accuracy in both feature selection and SVM optimization, as shown in Table 3 . When these features were used to train an optimized SVM, CHOA-based classification surpassed all other methods (Table 4). CHOA reduced the feature space by 69.4% (315/1,028 features), enhancing computational efficiency without sacrificing accuracy.

The proposed model' s classification performance for the three fuel plate types is detailed in Table 5 , demonstrating optimal accuracy (100%) for Regular plates with high performance maintained for remaining classes. The confusion matrix in Fig. 7 [FIGURE:7] and ROC curves in Fig. 8 [FIGURE:8] provide visual validation. The model correctly classified all 1,810 Regular and 1,496 Observed plate images. For the Defected class, only 1 out of 264 images was misclassified. ROC curves confirm robustness, with AUC values of 1.0 (Regular), 0.9967 (Observed), and 0.9985 (Defected), indicating strong discriminative power across all classes.

Comparative Analysis: Table 6 summarizes key studies in nuclear fuel plate inspection, emphasizing methodologies, datasets, and performance metrics. The proposed model advances existing approaches by integrating optimized feature selection with multi-class SVM classification, achieving superior accuracy and generalizability.

5. Conclusion

This study presented an advanced automated inspection system for evaluating U O -Al dispersion fuel plate homogeneity by integrating X-ray radiography, deep learning, and metaheuristic optimization. The framework leverages EfficientNet-B0 for robust deep feature extraction, followed by CHOA for optimal feature selection and SVM hyperparameter tuning. The system achieved 99.77% binary accuracy (Hom/Non-Hom) and 99.72% ternary accuracy (Regular/Observed/Defected), outperforming competing algorithms (SSA, WOA, GWO, DA, SCA). CHOA reduced features by 81.4% (binary) and 69.4% (ternary), enhancing computational efficiency without sacrificing accuracy. The model demonstrated near-perfect discriminative capability, with 100% accuracy for Regular plates and 99.72% for Defected plates, validated by AUC values of 1.0, 0.9967, and 0.9985 for respective classes. This approach addresses critical limitations of manual feature dependency, computational inefficiency, and over-

simplified binary classification, offering a fast, reliable, and automated solution for nuclear fuel quality assurance.

References

[1] W. Z. a. I. Elseaidy, "General Description and Production Lines Of The Egyptian Fuel Manufacturing Pilot Plant," in IGORR 7: 7th meeting of the International Group On Research Reactors, Germany, 1999.

[2] I. A. E. Agency, Standardization of Specifications and Inspection Procedures for Leu Plate-type Research Reactors (Report of A Consultants meeting, Geesthacht, 16-18 April 1986). Vienna: IAEA-TECDOC-467, IAEA, 1988.

[3] H. B. Peacock, "Properties of U O -aluminum cermet fuel," 01 October 1989. [Online]. Available: https://doi.org/10.2172/7262763

[4] K. L. Ali et al., "Development of low enriched uranium target plates by thermo-mechanical processing of UAl –Al matrix for production of Mo in Pakistan," *Nuclear Engineering and Design*, vol. 255, pp. 77-85, 2013.

[5] M. Durazzo, E. Vieira, E. F. Urano de Carvalho, and H. G. Riella, "Evolution of fuel plate parameters during deformation in rolling," *Journal of Nuclear Materials*, vol. 496, pp. 197-210, 2017.

[6] R. A. Salinas, U. Raff, and H. Coronado, "Uranium Density Measurements and Homogeneity Assessment in Quality Control of Low Enriched ^{23} U Fuel Plates Using Machine Vision,"*Measurement and Control*, vol. 36, no. 10, pp. 305-308, 2003.

[7] N. A. Mansour, M. E. El-Bedawy, and M. M. Ghoneim, "Effect of delay time between mixing and compacting for producing nuclear fuel plates," *Journal of Radiation Research and Applied Sciences*, vol. 14, no. 1, pp. 429-439, 2021.

[8] A. S. Elkorany and Z. F. Elsharkawy, "Efficient breast cancer mammograms diagnosis using three deep neural networks and term variance,"*Scientific Reports*, 2023.

[9] A. S. Elkorany and Z. F. Elsharkawy, "Optik COVIDetection-Net: A tailored COVID-19 detection from chest radiography images using deep learning," *Optik*, 2021.

[10] A. S. Elkorany and Z. F. Elsharkawy, "Automated optimized classification techniques for magnetic resonance brain images," *Multimedia Tools and Applications*, vol. 79, no. 37-38, pp. 27791-27814, 2020.

[11] A. S. Elkorany, M. Marey, K. M. Almustafa, and Z. F. Elsharkawy, "Breast Cancer Diagnosis Using Support Vector Machines Optimized by Whale Optimization and Dragonfly Algorithms," *IEEE Access*, vol. 10, 2022.

[12] Z. F. Elsharkawy, A. S. Elkorany, and S. M. Elhalafawy, "Deep Learning-Based Classification of Magnetic Resonance Brain Images," vol. 34, no. 2, 2025.

[13] H. M. Ahmed et al., "Hybridized classification approach for magnetic resonance brain images using gray wolf optimizer and support vector machine," *Multimedia Tools and Applications*, vol. 78, no. 19, pp. 27983-28002, 2019.

[14] H. M. Ahmed et al., "Hybrid gray wolf optimizer–artificial neural network classification approach for magnetic resonance brain images," *Applied Optics*, vol. 57, no. 7, pp. B25-B31, 2018.

[15] A. B. Gabis, Y. Meraihi, S. Mirjalili, and A. Ramdane-Cherif, "A comprehensive survey of sine cosine algorithm: variants and applications," *Artificial Intelligence Review*, vol. 54, 2021.

[16] A. S. Elkorany and Z. F. Elsharkawy, "Deep Learning Based Classification of Magnetic Resonance Brain Images using YOLOv5 and Lion Swarm Optimization," *Menoufia Journal of Electronic Engineering Research*, 2025.

[17] M. Khishe and M. R. Mosavi, "Chimp optimization algorithm," *Expert Systems with Applications*, 2020.

[18] W. Lei, K. Jia, X. Zhang, and Y. Lei, "Research on Chaotic Chimp Optimization Algorithm Based on Adaptive Tuning and Its Optimization for Engineering Application," *Journal of Sensors*, vol. 2023, 2023.

[19] S. Khosravi and A. Chalechale, "Chimp Optimization Algorithm to Optimize a Convolutional Neural Network for Recognizing Persian/Arabic Handwritten Words," *Mathematical Problems in Engineering*, vol. 2022, 2022.

[20] L. Deng and S. Liu, "Exposing the chimp optimization algorithm: A misleading metaheuristic technique with structural bias," *Applied Soft Computing*, vol. 158, 2024.

[21] S. Keyvan, X. Song, and M. Kelly, "Nuclear fuel pellet inspection using artificial neural networks," *Journal of Nuclear Materials*, vol. 264, no. 1, pp. 141-154, 1999.

[22] K. H. Mohamed et al., "Automated Image Analysis System for Homogeneity Evaluation of Nuclear Fuel Plates," in *2005 International Conference on Neural Networks and Brain*, 2005.

[23] Z. Guo et al., "Defect detection of nuclear fuel assembly based on deep neural network," *Annals of Nuclear Energy*, vol. 137, 2020.

[24] H. F. Aamir Khan, "Principal Component Analysis-Linear Discriminant Analysis Feature Extractor for Pattern Recognition," *International Journal of Computer Science Issues*, vol. 8, no. 6, pp. 267-270, 2011.

[25] P. Bansal et al., "Automatic detection of osteosarcoma based on integrated features and feature selection using binary arithmetic optimization algorithm," *Multimedia Tools and Applications*, vol. 81, no. 6, pp. 8807-8834, 2022.

[26] M. M. U. S. Shakin et al., "Squeeze and Excitation Attention Meets Modified EfficientNetB0 Architecture: Multi-Class Brain Tumor Classification Using

Explainable Artificial Intelligence," in *2023 26th International Conference on Computer and Information Technology*, 2023.

[27] C. Su and W. Wang, "Concrete Cracks Detection Using Convolutional Neural Network Based on Transfer Learning," *Mathematical Problems in Engineering*, vol. 2020, 2020.